



CEP55, serving as a diagnostic marker gene for osteosarcoma, triggers the JAK2-STAT3-MMPs axis

Yiqun Yan, MSc^{a,b}, Junyan He, MSc^{a,b}, Wendan Cheng, PhD^{a,b,*}

Background: Osteosarcoma (OS) stands as the prevailing form of primary bone cancer in clinical practice. Lack of effective treatment options and an overall poor prognosis are caused by the disease's exceptionally rare occurrence and unclear rationale.

Objective: This study's goal is to determine diagnostic marker genes involved in the progression of OS and investigate related pathways and mechanisms with the purpose of offering effective methods for OS diagnostics and therapy.

Methods: The Gene Expression Omnibus database provided the gene microarray data. Core genes were identified through differential expression analysis and WGCNA. Three techniques for machine learning, random forest, least absolute shrinkage and selection operator regression, and support vector machine recursive feature elimination, were used to further screen the core genes and obtain diagnostic marker genes for OS. The specificity and sensitivity of the diagnostic marker genes for OS diagnosis were evaluated using receiver operating characteristic curves. Western blotting analysis was used for preliminary validation of the diagnostic marker genes and their related pathways.

Results: Two diagnostic marker genes were identified through screening, including CEP55 and WWF. Receiver operating characteristic curves have been utilized to assess the diagnostic and therapeutic effects of CEP55 and WWF on OS. Western blotting analysis preliminarily validated the overexpression of CEP55 in OS and its capacity to control MMP2 and MMP9 levels by activating the JAK2/STAT3 signaling pathway.

Conclusion: At the first time, this research shows that CEP55 and WWF are more powerful diagnostic and predictive indicators for OS. CEP55 holds the capacity to activate the JAK2/STAT3 signaling pathway and modulate MMP2 and MMP9 levels, thereby positioning it as a promising target in OS treatment.

Keywords: bioinformatics, LASSO, osteosarcoma, RF, SVM-RFE, WGCNA

Introduction

Osteosarcoma (OS), being the prevailing form of primary bone cancer, has an unusually low incidence rate. According to incomplete statistics, the disease occurs in approximately 4.4 cases for each million people annually in kids and teens^[1]. However, the cause of OS in the majority of affected individuals is still unknown, leading to a lack of effective treatment options and a poor overall prognosis^[2]. Systemic neoadjuvant chemotherapy combined with surgical treatment remains the mainstay of therapy, and the necrosis rate of the resected tumor sample is considered a key prognostic indicator^[3]. However, with the

^aDepartment of Orthopedics and ^bInstitute of Orthopedics, Research Center for Translational Medicine, The Second Affiliated Hospital of Anhui Medical University, Hefei, Anhui province, People's Republic of China

Sponsorships or competing interests that may be relevant to content are disclosed at the end of this article.

*Corresponding author. Address: Second Affiliated Hospital of Anhui Medical University, Hefei 230601, Anhui province, People's Republic of China. Tel.: +86 13230651976. E-mail: chenwendan@ahmu.edu.cn (W. Cheng).

Copyright © 2023 The Author(s). Published by Wolters Kluwer Health, Inc. This is an open access article distributed under the terms of the Creative Commons Attribution-Non Commercial-No Derivatives License 4.0 (CCBY-NC-ND), where it is permissible to download and share the work provided it is properly cited. The work cannot be changed in any way or used commercially without permission from the journal.

Annals of Medicine & Surgery (2024) 86:190–198

Received 11 September 2023; Accepted 30 October 2023

Published online 7 November 2023

<http://dx.doi.org/10.1097/MS9.0000000000001491>

HIGHLIGHTS

- We have, for the first time, elucidated the crucial role of CEP55 in the activation of the JAK2-STAT3-MMPs axis in osteosarcoma (OS).
- We innovatively adopted three machine learning methods to screen core genes that are closely related to the development of OS, which makes the screened marker genes more diagnostic value.
- Preliminary evidence, derived from receiver operating characteristic curve modeling and Western blot analysis, suggests that the marker gene CEP55 holds promise as a potential therapeutic target for OS.

continuous advancement of clinical research, the practicality of this approach and its indicators in the treatment of OS have become increasingly controversial. This is because a considerable number of patients experience local recurrence, metastasis, or develop strong drug resistance after treatment^[4,5]. In the face of this phenomenon, it is necessary to explore more powerful diagnostic and predictive indicators^[6].

Recently, propelled by the advent of high-throughput sequencing technologies, research workers' understanding of biology and human diversity is undergoing unprecedented changes^[7]. Correspondingly, this has also driven the development of bioinformatics analysis in revealing pathogenic genes, exploring disease mechanisms, and other aspects^[8]. The detection and recognition of diagnostic biomarkers for OS have emerged as

the central focus of contemporary research. By studying these diagnostic biomarkers and their related pathways, it is possible to better predict the progression of patients' conditions and provide personalized diagnosis and treatment plans^[9–11].

In this work, firstly, we conducted preliminary screening and processing of samples from four GEO datasets by setting conditions. Then, using three machine learning methods, we obtained two diagnostic biomarkers including CEP55 and VWF. Finally, we found that the overexpression of CEP55 in OS prompts the activation of the JAK2/STAT3 signaling pathway, subsequently governing the expression of MMP2 and MMP9. These results demonstrate the diagnostic significance of CEP55 in OS and its potential as a viable therapeutic target.

Materials and methods

Data source and preprocessing

Collect and download three high-level OS microarray datasets from the Gene Expression Omnibus (GEO) database, including: GSE33382-GPL10295, GSE14827-GPL570, GSE21257-GPL10295, and one normal bone tissue microarray dataset GSE36001-GPL6102.

Based on the criteria: age less than 25 years old, presence or absence of metastasis, preliminary screening, and integration of samples from each high-level OS microarray dataset. In total, 117 samples were obtained, comprising 49 instances of primary OS and 68 instances of metastatic OS. Batch implications were mitigated through the utilization of the 'limma' package and the 'SVA' package. Standardized fusion of samples from the normal bone tissue dataset with primary and metastatic samples from the high-grade OS dataset, respectively, for further analysis^[12,13]. The integrated dataset of normal bone tissue samples (HC group) and primary OS samples (Primary OS group) is named G1, and the integrated dataset of normal bone tissue samples (HC group) and metastatic OS samples (Metastatic OS group) is named G2. For more details on the datasets, please refer to Table 1.

The acquisition of differentially expressed genes and the construction of co-expression networks

Employ the 'limma' package to discern genes with differential expression between the HC group and the primary OS group, as well as between the HC group and the metastatic OS group. The

criteria for selection are $P < 0.05$ and $|\log\text{FC}| > 1$. Visualize the results using the 'pheatmap' function.

The WGCNA package was used to construct gene co-expression networks of primary OS and normal bone tissue expression profiles, and metastatic OS and normal bone tissue expression profiles, respectively. Select an appropriate gene standard deviation value to filter gene sets for further analysis^[14]. Use the 'goodSampleGenes' function to ensure that there are no missing values or abnormal conditions in the dataset. Employ the 'pickSoftThreshold' function to establish the most suitable soft threshold and transform the gene expression data matrix into the corresponding adjacency matrix. Then, identify gene modules using the topological overlap clustering method. By calculating the module eigengenes and merging similar modules, a hierarchical clustering dendrogram is further generated. Evaluate gene significance and module significance based on the corresponding phenotype data to further demonstrate the significance between related genes and clinical information, as well as the correlation between modules and models.

Selection of diagnostic biomarkers and construction of diagnostic models

In the WGCNA results, modules that are significantly associated with the disease and have a P -value < 0.05 are considered central modules. Utilize the 'VennDiagram' package to conduct an intersection analysis between the genes exhibiting differential expression and those encompassed within the central modules^[15]. Use three machine learning algorithms, including random forest (RF), support vector machine recursive feature elimination, and least absolute shrinkage and selection operator (LASSO) regression, to further filter the genes obtained from the intersection^[16–18]. Take the intersection of the results from the three algorithms as the diagnostic signature genes for OS. Build a ROC curve and calculate the area under the ROC curve (AUC) to preliminarily evaluate the diagnostic significance of the signature genes.

Cell culture and transient transfection

The MG63 human OS cell line and CP-H111 human osteoblast was purchased from Wuhan Punoise Life Science and Technology Co., Ltd. in May 2023. The cells underwent relevant cell genetic testing and identification. The cells were grown in MEM medium supplemented with 10% fetal bovine serum, in a humidified incubator at 37°C and 5% CO₂.

The shRNA targeting CEP55, JAK2, and STAT3 were designed and constructed by China Shanghai Gemma Pharmaceuticals Co. The recombinant vectors and packaging vectors were co-transfected into MG63 cells using Lipofectamine 2000 (Invitrogen) to generate lentiviral particles. MG63 cells were cultured in a six-well plate and transfected with shCEP55, shJAK2, and shSTAT3 separately. Transfected cells were cultured for 5 days and the efficiency of target gene knockdown in this cell line was assessed by Western blotting analysis. The shRNA targeted sequences were as follows: (1) CEP55 shRNA: 5'-CCAGAAGTACCAAAGATT TAA-3'. (2) JAK2 shRNA: 5'-GCAGAATTAGCAAACCTTATA-3'. (3) STAT3 shRNA: 5'-TGTTCTCTATCAGCACAAT-3'.

Western blotting analyze

The cells were lysed using RIPA lysis buffer supplemented with protease inhibitors (Beyotime Biotech#P0013B). The proteins were separated by 6 or 10% SDS-PAGE and transferred onto

Table 1
Vital details of the microarray datasets included in this study.

| GEO series | Normal | Os_primary | Os_metastatic | Total number of samples |
|-------------------|--------|------------|---------------|-------------------------|
| GSE33382-GPL10295 | 0 | 16 | 31 | 47 |
| GSE14827-GPL570 | 0 | 17 | 9 | 26 |
| GSE21257-GPL10295 | 0 | 16 | 28 | 44 |
| GSE36001-GPL6102 | 4 | 0 | 0 | 4 |
| G1 | 4 | 49 | 0 | 53 |
| G2 | 4 | 0 | 68 | 72 |

PVDF membranes. sealing in 5% skimmed milk, the membranes were incubated with primary antibodies against CEP55 (1:1000, AB_2836271), STAT 3 (1:1000, AB_2835144), P-STAT 3 (1:1000, AB_2810278), MMP 9 (1:1000, AB_2837714), JAK 2 (1:1000, AB_2834956), P-JAK 2 (1:1000, AB_2834455), MMP 2 (1:1000, AB_2837815), JAK 1 (1:1000, AB_2834933), P-JAK 1 (1:1000, AB_2834437), FOXM1 (1:1000, AB_2838918), and GAPDH (1:3000, AB_2839421) overnight at 4°C. All antibodies were rabbit polyclonal antibodies from Affinity Bioreagents. The membranes were then incubated with secondary antibodies at 37°C for 2 h and the protein bands were visualized using a microplate chemiluminescence system (Share-BIO, SB-WB012). Subsequently, the bands were normalized and analyzed for each purpose using Image J, 1.80v software, using the GAPDH bands as the standard.

Results

Characterization of DEGs and identification of WGCNA key modules

Significant differences were observed between the primary OS group and the HC group, resulting in the identification of a total of 554 differentially expressed genes (DEGs). Among these, 147 genes exhibited significant downregulation, while 407 genes displayed significant upregulation (Fig. 1A). The optimal soft threshold $\beta = 4$ (scale-free $R^2 = 0.9$) was selected to construct a co-expression network between the two groups (Fig. 1E). By dynamic hybrid cutting, a total of 11 modules of different colors were obtained (Fig. 1C). The Pearson correlation coefficients and significance levels between each module and clinical traits were calculated and presented in a heatmap (Fig. 1G). Key modules were distinguished, consisting of the brown module comprising 276 genes and the yellow module comprising 220 genes.

Similarly, significant differences were observed between the metastatic OS group and the HC group, resulting in the identification of a total of 732 DEGs. Among these, 276 genes exhibited significant downregulation, while 456 genes displayed significant upregulation (Fig. 1B). The optimal soft thresholding power $\beta = 3$ (scale-free $R^2 = 0.9$) was chosen to construct a co-expression network between the two groups (Fig. 1F). By dynamic hybrid splicing, a total of 11 modules with different colors were obtained (Fig. 1D). The Pearson correlation coefficients and significance levels between each module and clinical traits were calculated and presented as a heatmap (Fig. 1H). Key modules were distinguished, consisting of the yellow module comprising 206 genes, the magenta module comprising 62 genes, the brown module comprising 316 genes, the pink module comprising 82 genes, and the red module comprising 120 genes.

The obtained DEGs were intersected with the genes in the key modules. This yielded a total of 49 core genes intimately linked to the onset and progression of OS (Fig. 2A).

Screening of diagnostic marker genes and the construction of diagnostic models

The obtained 49 core genes underwent additional screening utilizing three machine learning algorithms: RF, LASSO, and SVM. In the primary OS group and HC group, 13 feature genes with relative importance greater than 0.25 were obtained using the RF algorithm (Fig. 2B), including:

TYROBP, CXCL12, CD93, LBP, ITGB2, CEP55, VWF, PECAM1, ATP8B4, RRAGD, DNASE1L3, HERC5, and LCP1. In the metastatic OS group and HC group, 12 feature genes with relative importance greater than 0.2 were obtained using the RF algorithm (Fig. 2C), including: CEP55, SOX11, CD93, NECTIN3, VWF, ITGB2, JCHAIN, ATP8B4, HLA.B, HLA.DRA, RNASE1, and TFF3. Then, the intersection of the two RF results was obtained, resulting in five intersecting genes: CD93, ITGB2, CEP55, VWF, and ATP8B4.

In both the primary OS group and the HC group, by employing the LASSO algorithm and 10-fold cross-validation, the amount of genes associated with the lowest cross-validation error (Fig. 2D) was identified as 9, encompassing CD93, CEP55, DNASE1L3, LBP, LCP1, NECTIN3, RRAGD, TF, and VWF. Similarly, in the metastatic OS group and HC group, through the LASSO algorithm (Fig. 2E), a total of 11 feature genes were determined, including ACKR1, ATP8B4, CEP55, CXCL12, DNASE1L3, LBP, LCP1, RRAGD, TF, TFF3, and VWF. Subsequently, the intersection of the two LASSO results yielded seven common genes, including CEP55, DNASE1L3, LBP, LCP1, RRAGD, TF, and VWF.

In the primary OS group and HC group, through the SVM algorithm and 10-fold cross-validation, the amount of genes associated with the lowest cross-validation error (Fig. 2F) was identified as 8, encompassing RRAGD, LAPTM5, VWF, JCHAIN, NECTIN3, LCP1, CEP55, and ITGB2. Similarly, in the metastatic OS group and HC group, through the SVM algorithm (Fig. 2G), a total of seven feature genes were determined, including RRAGD, VWF, CEP55, TYROBP, LAPTM5, AQP1, and LCP1. Subsequently, the intersection of the two SVM results yielded five common genes, including RRAGD, LAPTM5, VWF, LCP1, and CEP55. Finally, the intersection genes of all the algorithms were crossed again (Fig. 2H) to obtain two diagnostic marker genes, including, VWF and CEP55.

For the purpose of determining the sensitivity as well as specificity of VWF and CEP55 in the OS diagnosis, ROC curves, and AUC values were utilized. It can be seen that the AUC values of the ROC curves for the two diagnostic marker genes in the primary OS group and HC group were 0.934, while the AUC values when used individually as diagnostic marker genes were 0.908 and 0.898, respectively (Fig. 3C). In the metastatic OS group and HC group, the AUC values of the ROC curves for the two diagnostic marker genes were 0.941, while the AUC values when used individually as diagnostic marker genes were 0.952 and 0.873, respectively (Fig. 3D). In addition, the expression of VWF and CEP55 in the primary OS group and HC group (Fig. 3A) as well as in the metastatic OS group and HC group (Fig. 3B) and the corresponding results were demonstrated with a box plot.

The diagnostic marker gene CEP55 promotes the expression of MMPs in OS cells

Prior research has demonstrated that CEP55 can expedite the invasion and metastasis of pancreatic cancer by fostering the upregulation of MMPs^[19]. Based on this, we propose that CEP55, as a diagnostic marker gene for OS, may also increase its invasion and metastasis ability by promoting the expression of MMPs in OS. Therefore, we used Western blot analysis to preliminarily validate the expression of relevant genes in normal bone tissue cells (HC), OS cells, and OS cells with CEP55 knockdown (shCEP55) (Fig. 4A, B). The findings

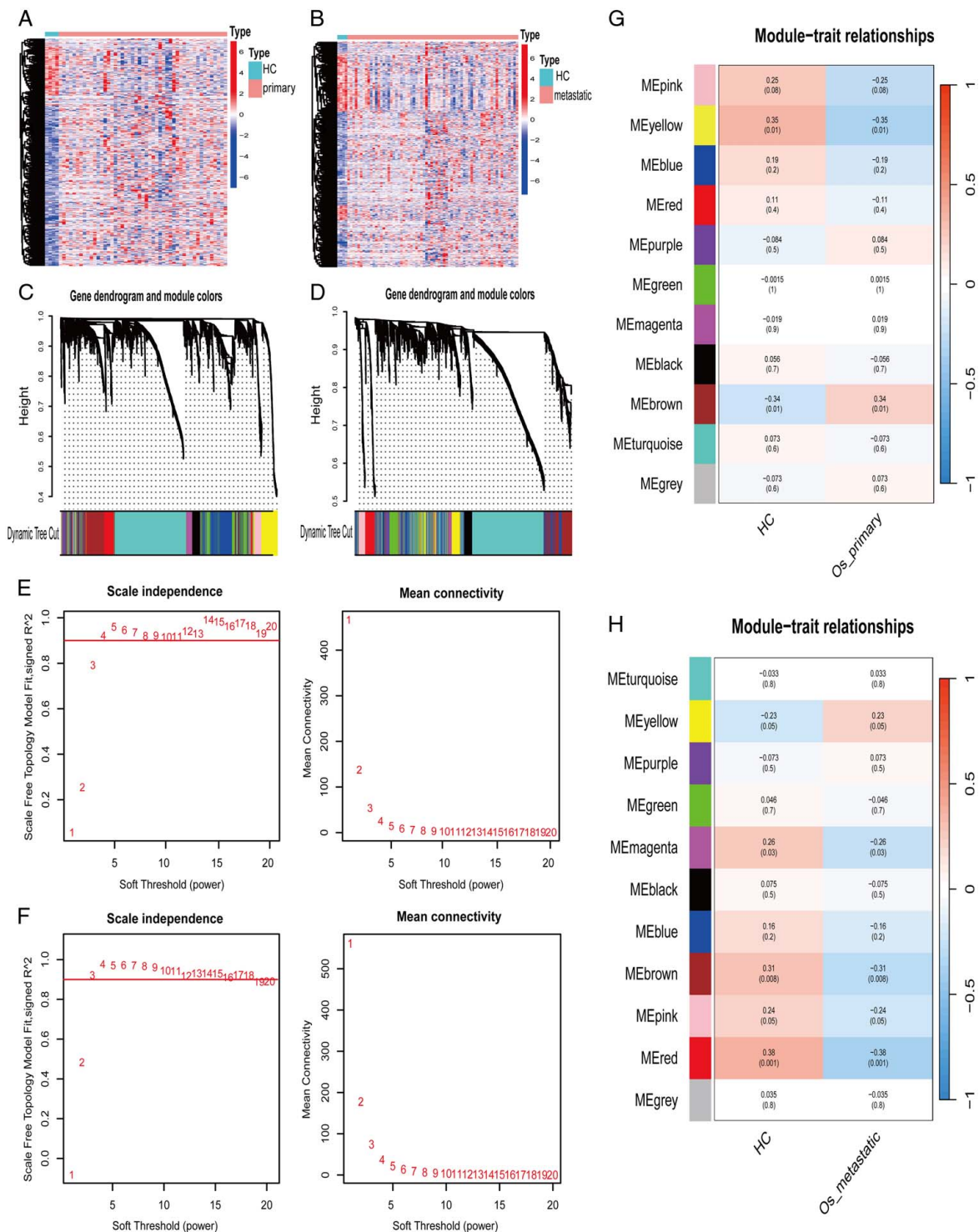


Figure 1. Expression of DEGs and WGCNA analysis. (A, B) Heatmap depicting the expression patterns of DEGs in primary OS and HC, as well as in metastatic OS and HC. (C) Hierarchical clustering dendrogram of primary OS and HC. (D) Hierarchical clustering dendrogram of metastatic OS and HC. (E) Scale-free fitting indices and average connectivity corresponding to the co-expression networks of primary OS and HC at different soft threshold powers. (F) Scale-free fitting indices and average connectivity corresponding to the co-expression networks of metastatic OS and HC at different soft threshold powers. (G, H) Heatmap showing the relationship and importance between clinical features and modules.

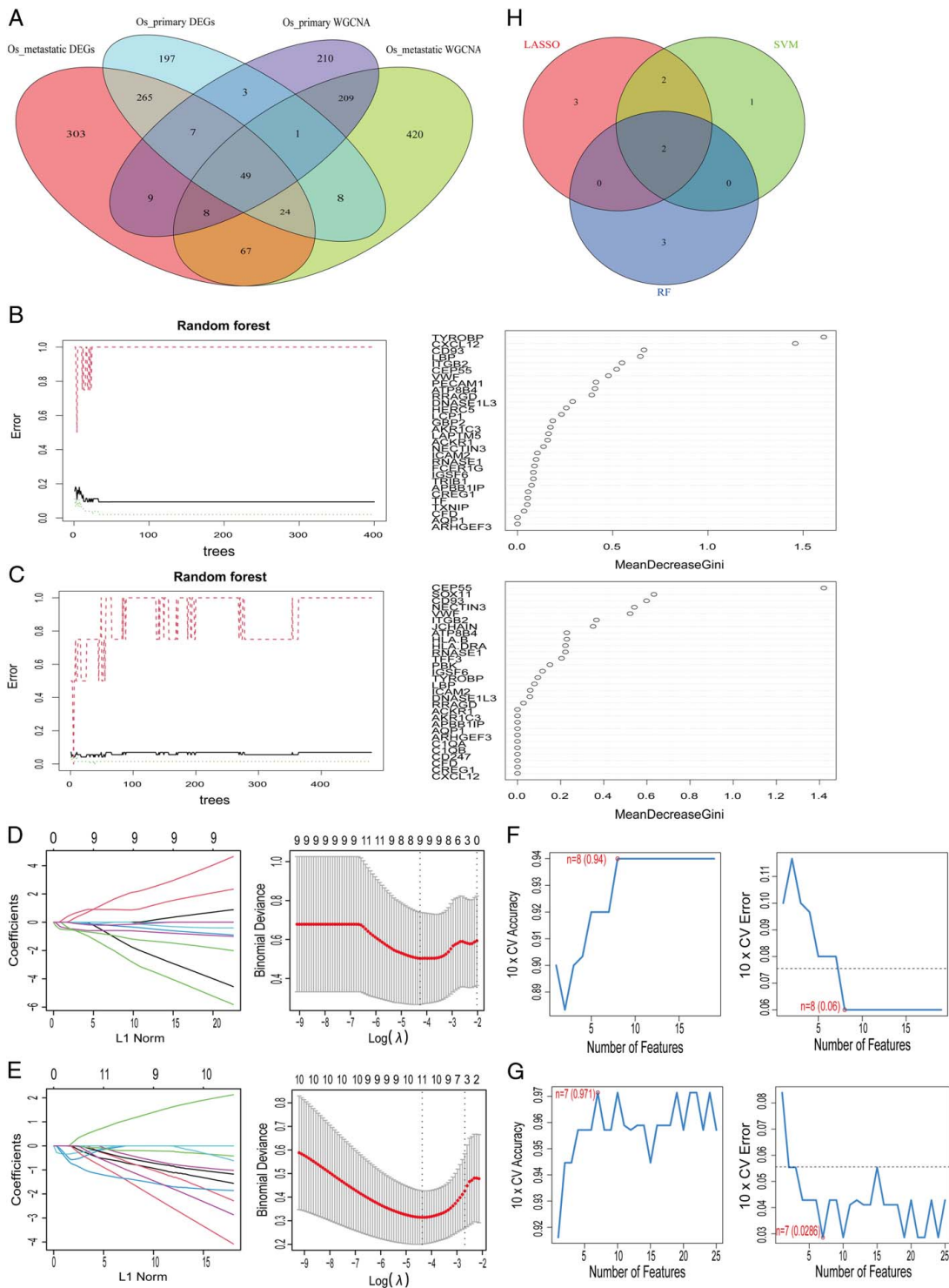


Figure 2. Feature gene selection using the RF algorithm, LASSO regression and SVM algorithm. (A) Intersection of DEGs and genes in the WGCNA key modules. (B, C) Relationship between the number of trees and the error rate, as well as the ranking of gene importance. (D, E) LASSO models and coefficient curves for 10-fold cross-validation. The vertical dashed line corresponds to the optimal lambda value. (F, G) Accuracy and cross-validation error curves for SVM. (H) Venn diagram of the three algorithm results.

revealed that in comparison to the HC group, CEP55 expression in the OS group exhibited a significant increase, aligning with the earlier data analysis, and MMP2 and MMP9 expression also demonstrated corresponding increases. Furthermore, when compared to the OS

group, CEP55 expression in the shCEP55 group exhibited a notable reduction, confirming the successful functional suppression mediated by shRNA. Additionally, MMP2 and MMP9 expression were substantially decreased. These results demonstrate that the diagnostic

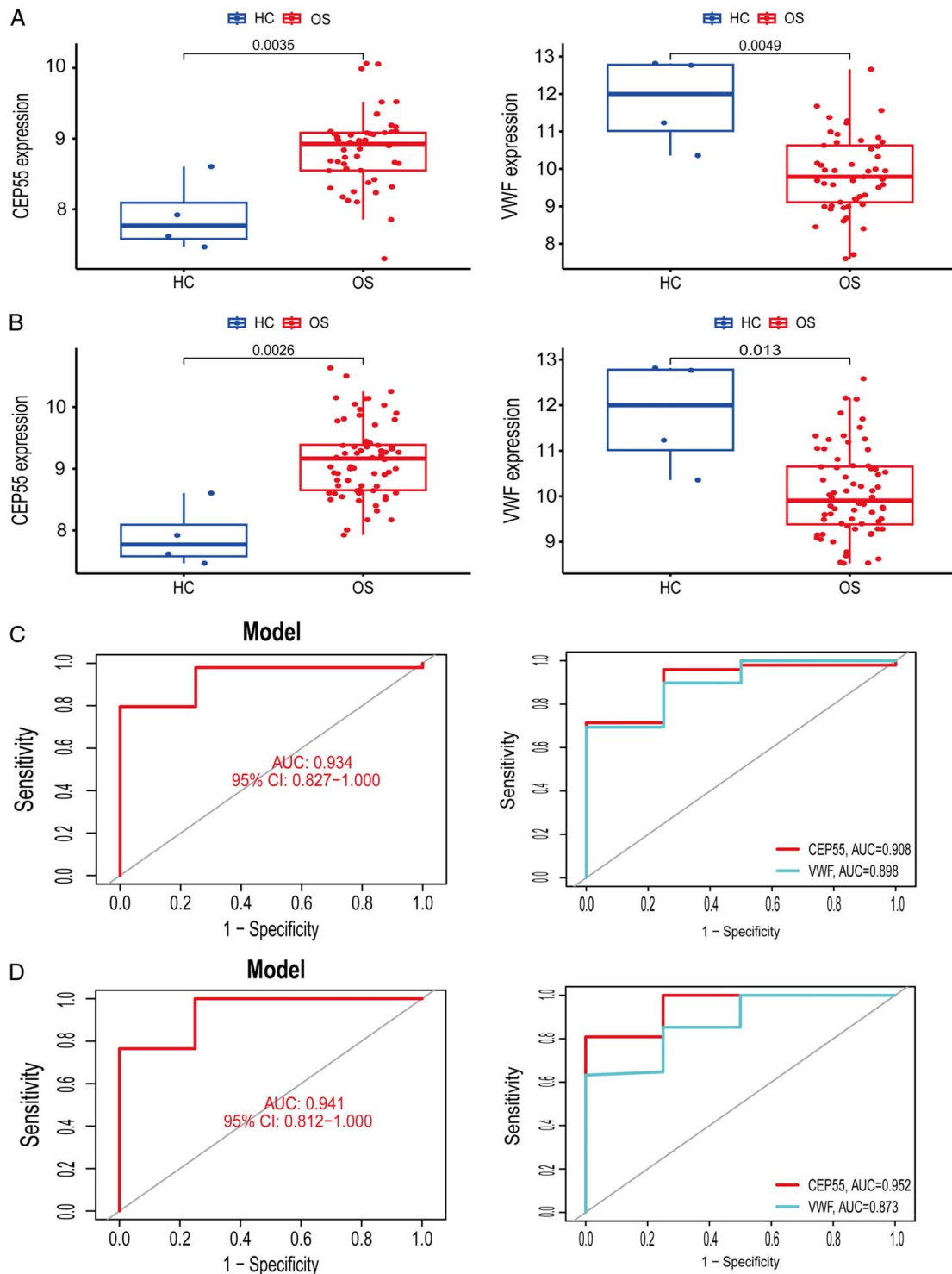


Figure 3. Expression and diagnostic value of CEP55 and VWF in osteosarcoma. (A, C) Expression differences and corresponding ROC curves of CEP55 and VWF in the primary OS group and HC group. (B, D) Expression differences and corresponding ROC curves of CEP55 and VWF in the metastatic OS group and HC group.

marker gene CEP55 can promote MMP2 and MMP9 expression in OS cells. However, intriguingly, MMP2 and MMP9 expression in the shCEP55 group remained elevated compared to those in the HC, suggesting that MMPs expression in OS is also regulated by other genes or factors.

CEP55 activates the JAK2-STAT3-MMP axis in OS cells

During the course of cancer migration and invasion, a range of extracellular factors, encompassing cytokines, growth factors, and interactions with neighboring cells, exert regulatory effects on the

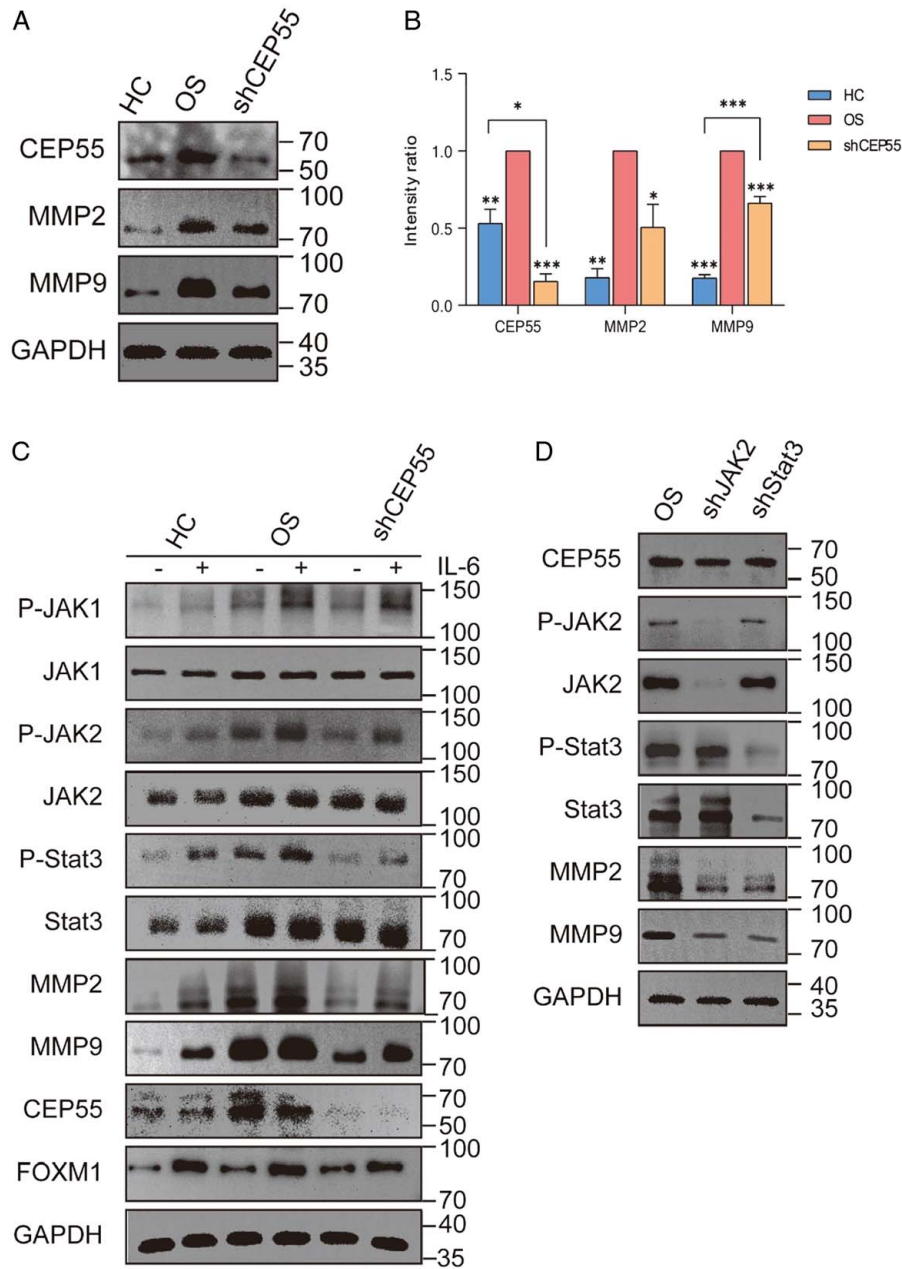


Figure 4. Stimulation of the JAK2/STAT3 signaling pathway by CEP55 promotes MMPs expression in OS. (A) Western blot analysis of CEP55, MMP2, and MMP9 in HC group, OS group, and shCEP55 group. (B) Quantitative histogram of Western blot analysis. (C) Western blotting analysis of relevant protein expression in the HC group, OS group, and shCEP55 group with or without incubation with 20 ng/ml IL-6 for 30 min. (D) Western blotting analysis of relevant protein expression in the OS group, the shJAK2 group, and the shSTAT3 group.

expression levels of MMPs^[20]. Studies have shown that IL-6 can enhance MMP2 and MMP9 expression through activation of the JAK/STAT3 signaling pathway^[21,22]. Based on this, we speculate that the reason CEP55 stimulates MMPs expression in OS may be that CEP55 is involved in the regulation of IL-6 and its downstream signaling pathways, which has been confirmed in hepatocellular carcinoma^[23]. Subsequently, we used IL-6 as an inducer to preliminarily validate this idea (Fig. 4C). Western blot analysis revealed that in comparison to the HC, the OS, and the shCEP55 group without IL-6 induction, the application of IL-6 markedly heightened MMP2, MMP9, and FOXO1 expression through

activation of the JAK/STAT3 signaling pathway. In addition, in the OS group with high expression of CEP55, regardless of whether IL-6 induction was used or not, compared with the corresponding shCEP55 group, we observed that JAK1, P-JAK1, JAK2, STAT3, and FOXM1 expression were basically consistent between the two groups. However, P-JAK2, P-STAT3, MMP2, and MMP9 expression in the OS was notably greater compared to that in the shCEP55 group. These results suggest that the overexpression of CEP55 promotes the phosphorylation of JAK2 and STAT3, whereas the suppression of CEP55 inhibits the IL-6-induced phosphorylation of JAK2 and STAT3. To further validate, we

suppressed JAK2 and STAT3 expression in OS cells and established the OS group, the shJAK2 group, and the shSTAT3 group (Fig. 4D). The findings revealed a marked decrease in JAK2, P-JAK2, MMP2, and MMP9 expression in the shJAK2 group compared to the OS group, while STAT3 and P-STAT3 remained unaffected. Similarly, there was a marked decrease in STAT3, P-STAT3, MMP2, and MMP9 expression in the shSTAT3 group compared to the OS group, while JAK2 and P-JAK2 remained unaffected. All these results indicate that CEP55 regulates MMP2 and MMP9 expression through activation of the JAK2/STAT3 signaling pathway in OS.

Discussion

So far, the causes of OS, the most common primary bone cancer in clinical practice, are still largely unknown and uncertain. Although some studies have suggested a higher incidence of OS in genetic cases with mutations in tumor suppressor genes^[24,25], these findings have not provided novel and effective means for the treatment of OS. Unfortunately, the traditional and conservative treatment approach of systemic chemotherapy combined with surgical resection has not changed consistently for more than three decades^[26]. While this approach has improved survival outcomes at the 5-year mark to over 65% in patients with localized tumors, the corresponding 5-year overall survival rate for those with metastatic tumors remains notably low, standing at less than 25%^[27,28]. This suggests that exploring new treatment modalities for OS and providing personalized diagnosis and treatment plans for patients is an inevitable trend. Due to the advancement of high-throughput sequencing technology and the increasing diversity of bioinformatics analysis methods, genomic data can be employed to precisely identify marker genes strongly associated with the onset and progression of diseases^[29,30]. By studying these marker genes and their related pathways, personalized treatments can be implemented for different patients.

In this study, considering that OS is more common in the population under 25-year-old, with a peak incidence at 18-year-old^[28], we selected samples with age less than 25 years from the GEO dataset for further analysis, which would make the results of the data analysis more accurate. Based on this, we constructed two datasets, G1 and G2, according to whether OS had metastasized. Subsequently, we performed DEGs screening and WGCNA analysis on the two datasets separately and intersected all the genes included in the corresponding results, resulting in 49 core genes that were significantly associated with OS and had differential expression compared to normal bone tissue. Then, we used three machine learning algorithms, RF, LASSO, and SVM, to further screen the 49 core genes in the G1 and G2 datasets and intersected all the genes included in the corresponding results again, resulting in two diagnostic marker genes: CEP55 and VWF. It can be seen that in relation to the HC, CEP55 expression was noticeably rising in the primary OS group ($P=0.0035$), and VWF expression was substantially declining ($P=0.0049$). Within the metastatic OS, CEP55 expression was noticeably rising ($P=0.0026$), and VWF expression was substantially declining ($P=0.013$). This suggests that the overexpression of CEP55 and the suppression of VWF expression could contribute to the initiation and progression of OS. To evaluate the specificity and sensitivity of VWF and CEP55 in the diagnosis of OS, we constructed ROC curve models. It can be seen that in the primary OS group and HC group, the AUC values of the ROC curves for both genes were 0.934, while the AUC values as

diagnostic marker genes alone were 0.908 and 0.898, respectively. In the metastatic OS group and HC group, the AUC values of the ROC curves for both genes were 0.941, while the AUC values as diagnostic marker genes alone were 0.952 and 0.873, respectively. These results confirm that VWF and CEP55 are strong diagnostic and predictive indicators of OS.

In the process of tumor progression, the increased expression of MMPs plays a crucial role. It can promote tumor angiogenesis, invasion, and metastasis, leading to a shorter survival time for patients^[31]. Prior research has shown that CEP55 can promote the expression of MMPs in pancreatic cancer cells, thereby accelerating the process of invasion and metastasis^[19]. Based on this, we propose that CEP55 may also promote the expression of MMPs in OS. Western blotting analysis and quantitative images indicated that CEP55 expression was noticeably rising in the OS group, with MMP2 and MMP9 expression also rising accordingly. Within the shCEP55 group, CEP55 expression experienced a substantial decline, and MMP2 and MMP9 expression experienced a substantial decline. These results demonstrate that CEP55 can promote MMP2 and MMP9 expression in OS. In the process of cancer cell migration and invasion, the expression of MMPs is regulated by various extracellular factors, among which IL-6 can enhance MMP2 and MMP9 expression through activation of the JAK/STAT3 signaling pathway^[21,22]. So, we speculate that the reason CEP55 stimulates MMPs expression in OS may be that CEP55 is involved in the regulation of IL-6 and its downstream signaling pathways. Subsequently, we conducted preliminary verification of this idea using IL-6 as an inducer. Western blot analysis revealed that in comparison to the HC, the OS, and the shCEP55 group without IL-6 induction, the application of IL-6 markedly heightened MMP2, MMP9, and FOXO1 expression through activation of the JAK/STAT3 signaling pathway. In the OS group with high expression of CEP55, regardless of whether IL-6 induction was used or not, compared with the corresponding shCEP55 group. However, P-JAK2, P-STAT3, MMP2, and MMP9 expression in the OS was notably greater compared to that in the shCEP55 group. These results suggest that the overexpression of CEP55 promotes the phosphorylation of JAK2 and STAT3, whereas the suppression of CEP55 inhibits the IL-6-induced phosphorylation of JAK2 and STAT3. Furthermore, FOXM1 expression in the HC showed a substantial decline compared to the other two groups, and it seemed to be unaffected by CEP55 expression. Next, we knocked down JAK2 and STAT3 expression in OS and monitored MMP expression. Western blotting analysis revealed a marked decrease in JAK2, P-JAK2, MMP2, and MMP9 expression in the shJAK2 group compared to the OS group, while STAT3 and P-STAT3 remained unaffected. Similarly, in shSTAT3, STAT3, P-STAT3, MMP2, and MMP9 expression were in substantial decline, while JAK2 and P-JAK2 were unaffected. All these results indicate that CEP55 regulates MMP2 and MMP9 expression through activation of the JAK2/STAT3 signaling pathway in OS. Hence, directing attention towards CEP55 might present a fresh avenue for suppressing the JAK2/STAT3 axis. Nevertheless, additional investigations are warranted to unveil the precise mechanisms through which CEP55 triggers associated molecules in vivo.

Conclusion

Within this investigation, we discovered two diagnostic marker genes for OS, CEP55, and VWF. Additionally, we demonstrated

for the first time that CEP55 in OS can regulate MMP2 and MMP9 expression through activation of the JAK2/STAT3 signaling pathway. This suggests that CEP55 may be associated with the advancement of the disease and an unfavorable prognosis in OS patients. Moreover, this underscores the significance of CEP55 as a potential target for clinical intervention.

Ethical approval

Not applicable.

Consent

Not applicable.

Sources of funding

Not applicable.

Author contribution

Y.Y.: completed the experiments and manuscript writing; J.H.: completed the data collection; W.C.: provided experimental guidance.

Conflicts of interest disclosure

The authors declare that they have no competing interests.

Research registration unique identifying number (UIN)

Not applicable.

Guarantor

Yiqun Yan.

Data availability statement

The datasets generated and/or analyzed during the current study are available in the GEO database (<https://www.ncbi.nlm.nih.gov/geo>).

Provenance and peer review

Not applicable.

References

- [1] Gill J, Gorlick R. Advancing therapy for osteosarcoma. *Nat Rev Clin Oncol* 2021;18:609–24.
- [2] Mirabello L, Kostler R, Moriarity BS, *et al.* A genome-wide scan identifies variants in NFIB associated with metastasis in patients with osteosarcoma. *Cancer Discov* 2015;5:920–31.
- [3] Hattinger CM, Bignon P, Iacoboni E, *et al.* Candidate germline polymorphisms of genes belonging to the pathways of four drugs used in osteosarcoma standard chemotherapy associated with risk, survival and toxicity in non-metastatic high-grade osteosarcoma. *Oncotarget* 2016;7:61970–87.
- [4] Fu Y, Lan T, Cai H, *et al.* Meta-analysis of serum lactate dehydrogenase and prognosis for osteosarcoma. *Medicine* 2018;97:e0741.
- [5] Herea D-D, Danceanu C, Radu E, *et al.* Comparative effects of magnetic and water-based hyperthermia treatments on human osteosarcoma cells. *Int J Nanomed* 2018;13:5743–51.
- [6] Xu J, Xie L, Guo W. Neoadjuvant chemotherapy followed by delayed surgery: is it necessary for all patients with nonmetastatic high-grade pelvic osteosarcoma?. *Clin Orthop Relat Res* 2018;476:2177–86.
- [7] Yang J, Zhang A, Luo H, *et al.* Construction and validation of a novel gene signature for predicting the prognosis of osteosarcoma. *Sci Rep* 2022;12:1279.
- [8] Pareek CS, Smoczynski R, Tretyn A. Sequencing technologies and genome sequencing. *J Appl Genet* 2011;52:413–35.
- [9] Liu W, Xie X, Qi Y, *et al.* Exploration of immune-related gene expression in osteosarcoma and association with outcomes. *JAMA Netw Open* 2021;4:e2119132.
- [10] Lyskjær I, Kara N, De Noon S, *et al.* Osteosarcoma: novel prognostic biomarkers using circulating and cell-free tumour DNA. *Eur J Cancer* 2022;168:1–11.
- [11] Yu Y, Wang L, Li Z, *et al.* Long noncoding RNA CRNDE functions as a diagnostic and prognostic biomarker in osteosarcoma, as well as promotes its progression via inhibition of miR-335-3p. *J Biochem Mol Toxicol* 2021;35:e22734.
- [12] Leek JT, Johnson WE, Parker HS, *et al.* The sva package for removing batch effects and other unwanted variation in high-throughput experiments. *Bioinformatics* 2012;28:882–3.
- [13] Ritchie ME, Phipson B, Wu D, *et al.* limma powers differential expression analyses for RNA-sequencing and microarray studies. *Nucleic Acids Res* 2015;43:e47.
- [14] Langfelder P, Horvath S. WGCNA: an R package for weighted correlation network analysis[J]. *BMC Bioinform* 2008;9:559.
- [15] Chen H, Boutros PC. VennDiagram: a package for the generation of highly-customizable Venn and Euler diagrams in R. *BMC Bioinform* 2011;12:35.
- [16] Liaw A, Wiener M. Classification and regression by randomForest. *R News* 2002;2:18–22.
- [17] Huang S, Cai N, Pacheco PP, *et al.* Applications of support vector machine (svm) learning in cancer genomics. *Cancer Genomics Proteomics* 2018;15:41–51.
- [18] Friedman J, Tibshirani R, Hastie T. Regularization paths for generalized linear models via coordinate descent. *J Stat Softw* 2010;33:1–22.
- [19] Peng T, Zhou W, Guo F, *et al.* Centrosomal protein 55 activates NF- κ B signalling and promotes pancreatic cancer cells aggressiveness. *Sci Rep* 2017;7:5925.
- [20] Bassiouni W, Ali MAM, Schulz R. Multifunctional intracellular matrix metalloproteinases: implications in disease. *FEBS J* 2021;288:7162–82.
- [21] Huang C, Yang G, Jiang T, *et al.* Effects of IL-6 and AG490 on regulation of Stat3 signaling pathway and invasion of human pancreatic cancer cells in vitro. *J Exp Clin Cancer Res* 2010;29:51.
- [22] Liu Q, Li G, Li R, *et al.* IL-6 promotion of glioblastoma cell invasion and angiogenesis in U251 and T98G cell lines. *J Neurooncol* 2010;100:165–76.
- [23] Li M, Gao J, Li D, *et al.* CEP55 promotes cell motility via JAK2–STAT3–MMPs cascade in hepatocellular carcinoma. *Cells* 2018;7:99.
- [24] Arndt CAS, Rose PS, Folpe AL, *et al.* Common musculoskeletal tumors of childhood and adolescence. *Mayo Clin Proc* 2012;87:475–87.
- [25] Lv Y, Wu L, Jian H, *et al.* Identification and characterization of aging/senescence-induced genes in osteosarcoma and predicting clinical prognosis. *Front Immunol* 2022;13:997765.
- [26] Whelan JS, Davis LE. Osteosarcoma, chondrosarcoma, and chordoma. *J Clin Oncol* 2018;36:188–93.
- [27] Meltzer PS, Helman LJ. New horizons in the treatment of osteosarcoma. *N Engl J Med* 2021;385:2066–76.
- [28] Beird HC, Bielack SS, Flanagan AM, *et al.* Osteosarcoma. *Nat Rev Dis Primers* 2022;8:77.
- [29] Zhang A, Yang J, Ma C, *et al.* Development and validation of a robust ferroptosis-related prognostic signature in lung adenocarcinoma. *Front Cell Dev Biol* 2021;9:616271.
- [30] Wang Y, Zhou C, Luo H, *et al.* Prognostic implications of immune-related eight-gene signature in pediatric brain tumors. *Braz J Med Biol Res* 2021;54:e10612.
- [31] Buttacavoli M, Di Cara G, Roz E, *et al.* Integrated multi-omics investigations of metalloproteinases in colon cancer: focus on MMP2 and MMP9. *Int J Mol Sci* 2021;22:12389.